Received: 31 March 2022 | Accepted: 2 September 2022
DOI: 10.1111/srt.13204

ORIGINAL ARTICLE

WILEY

Robust skin microrelief depth estimation using a mobile stereo system

Cho-I Moon[1] | Onseok Lee[1,2] | Min-Hyung Choi[3]

[1]Department of Software Convergence, Graduate School, Soonchunhyang University, Asan, Chungnam, Republic of Korea

[2]Department of Medical IT Engineering, College of Medical Sciences, Soonchunhyang University, Asan, Chungnam, Republic of Korea

[3]Department of Computer Science and Engineering, College of Engineering, Design and Computing, University of Colorado Denver, Denver, Colorado, USA

Correspondence
Onseok Lee, Department of Medical IT Engineering, College of Medical Sciences, Soonchunhyang University, 22, Soonchunhyang-ro, Asan 31538, Chungnam, Republic of Korea.
Email: leeos@sch.ac.kr

Abstract

Background: The skin surface becomes wrinkled and rough due to various internal and external factors. A three-dimensional (3D) analysis of the skin is required to improve skin conditions. Stereophotogrammetry, a noninvasive 3D analysis method, is easy to install and use, but most stereo systems have a fixed baseline and scale. Previous stereo systems are not suitable for observing micro-range skin features. Therefore, we suggest the optimal conditions and methods for the 3D analysis of skin microrelief using a multi-conditioned stereo system.

Methods: We constructed a nonconvergence model using a mobile device and acquired stereo images under multiscale and multi-baseline conditions. We extracted 3D information of the skin through our process: preprocessing, skin feature extraction, feature matching, and actual depth mapping. We improved the accuracy of the 3D analysis of the skin by using disparity values instead of disparity maps. We compared and analyzed the performances of six local feature detector and descriptor algorithms. In addition, we suggested depth-mapping formulas to estimate the actual depth of the skin microrelief.

Results: We confirmed that stereo images with a working distance of 70–75 mm and a baseline of 4–8 mm are effective for the 3D analysis of skin microrelief. In addition, accelerated KAZE exhibited the best performance for features extraction and stereo matching. Finally, the extracted 3D information was converted to the actual depth, and the performance of the 3D analysis was verified.

Conclusion: The proposed system and method that provide texture information are effective for 3D skin disease analysis and evaluation.

KEYWORDS
mobile stereo system, optimization, skin three-dimensional analysis, stereo matching

1 | INTRODUCTION

Skin is the largest organ in the body and is a mechanically complex material composed of multiple layers of various components. Various internal and external factors cause changes in the physical and material properties of the internal structure of the skin and morphological and topological properties of the epidermis such as wrinkles. Skin topography is represented by microrelief (roughness) and macro-relief (wrinkles).[1] Skin roughness and wrinkles are hallmarks of aging and play a key role in the analysis of skin conditions. Skin microrelief is composed of a network of furrows and ridges formed by unstructured polygonal patterns.[2] During aging, the replacement rate of keratinocytes is reduced, collagen fibers are destroyed, and the substrate of the dermis is reduced. Therefore, the skin loses elasticity and sags, and the wrinkles deepen, resulting in a change in skin topography.[3,4] Accurate skin evaluation is required to alleviate skin microrelief that is roughened by dramatic changes due to aging and disease[5]; in particular, a three-dimensional (3D) analysis of the skin is essential for accurate treatment.

Among noninvasive 3D imaging techniques, stereophotogrammetry extracts the 3D information of an object using images acquired from two or more viewpoints. It extracts identical features from stereo images of different views, matches them, and then estimates depths through triangulation. Stereophotogrammetry can be used in clinical environments because of its fast image acquisition, simple calibration, and relatively inexpensive and reliable hardware.[6–8] Previous 3D skin studies had generated a disparity map, representing the 3D information, using structured equipment and software,[9] or analyzed 3D information such as the width and depth of the skin wrinkles using only a two-dimensional (2D) skin image.[10,11] However, the disparity map of the skin surface cannot easily express its microstructure, and the procedure requires a large time period. In addition, a 3D analysis of the skin surface using 2D skin images lacks accuracy and precision. Moreover, the 3D analysis equipment and methods used in clinical studies have limitations in terms of practicality and universality owing to their high cost, considerable expertise, and time consumption.

Recently, as the hardware performance of mobile devices has improved, various studies have utilized high-resolution images acquired using mobile cameras.[12–14] Mobile cameras are easy to use and install and can be used in multiple ways in the field of healthcare. Therefore, we acquired stereo images of the skin surface using a mobile device and performed a 3D analysis of skin microrelief through feature extraction and stereo matching. We acquired multi-conditioned stereo images (multiscale, multi-baseline) and suggested optimal stereo conditions for skin surface analysis.

In addition, we used stereo matching algorithms of the local approach to estimate the skin microrelief depth in a given left/right skin image. We analyzed the micro-range depth of the skin images. To date, few studies have extracted meaningful features and matched them. In addition, in the case of skin surface images, which include dynamic changes, the skin surface structure consists of a collection of polygons with similar intensities, shapes, and sizes. Numerous matching errors occur owing to the effects of noises such as skin surface color differences and reflections. These difficulties are particularly evident in mobile skin image. Therefore, we evaluated the performance of the feature extraction and matching algorithms for illumination, translation, scale, rotation, and viewpoint changes. We compared the following stereo matching algorithms based on local feature extraction in mobile skin images: SIFT,[15] SURF,[16] BRISK,[17] ORB,[18] ASIFT,[19] and accelerated KAZE (AKAZE).[20] Finally, we suggested a depth-mapping formula for stereo matching using standard scalar bar images. We analyzed the 3D information of the skin microrelief using the disparity values obtained using the optimal conditioned stereo images. In addition, excluding the existing disparity maps generation with large errors, we performed an accurate and precise 3D analysis of the skin using 3D points for skin microrelief features. Our study suggested optimal conditions for 3D depth estimation of a wide-view skin image and a fast and accurate analysis process.

2 | MATERIALS AND METHODS

2.1 | Skin microrelief stereo images

2.1.1 | Subjects

We acquired mobile images of skin in the dorsal hand of eight healthy subjects in the 20-year age group. The skin in the dorsal hand can detect the morphological and topological changes in the network of skin microrelief and observe the curvature caused by sagging of aging skin. The subjects were selected after confirming that they did not have any skin disease and nonsmoker. This study was carried out in accordance with the ethical principles of the Helsinki Declaration and approved by the Institutional Review Board. Written informed consent was obtained from all participants in the experiment (No. 1040875-202002-BM-009).

2.1.2 | Multi-conditioned mobile stereo system

For our stereo system, we used a Galaxy A3 (SM-A310NZKAKOO, Samsung Electronics Co., Suwon, South Korea; rear camera: 1.3 MP, aperture: F1.9). We acquired images (magnification: 2.0×; ratio: 4:3) of the skin surface of the dorsal hand.

Existing 3D skin studies using the stereo vision technique were based on stereo images with a fixed scale and baseline.[1] However, the disparity, which is depth information, is represented differently depending on the changes in the scale of the stereo images and the baseline (the distance between the optical axes of the two cameras). A wider disparity range provides more precise 3D skin analysis. Therefore, it is necessary to select suitable conditions, scale, and baseline stereo images to enable precise disparity representation of the observation area. We can acquire wide-view images at various scales and baselines using a mobile device. We installed the mobile camera to be perpendicular to the shooting direction and acquired stereo images with a right and left view by shifting the camera in the same horizontal line. To acquire a mobile image capable of detecting skin fine features such as wrinkles and wrinkled cells as well as observing a wider area of skin, we set the working distance to 60–80 mm. The working distance was adjusted at 5-mm intervals and photographed at a total of five steps working distances. At each working distance, the baseline of the stereo image was adjusted through 10 steps by moving the camera at intervals of 1 mm to the left in the range of 1–10 mm. In the boundary region of the skin on the back of the hand, the polynomial pattern of the skin microstructure is deformed by the curvature. For an

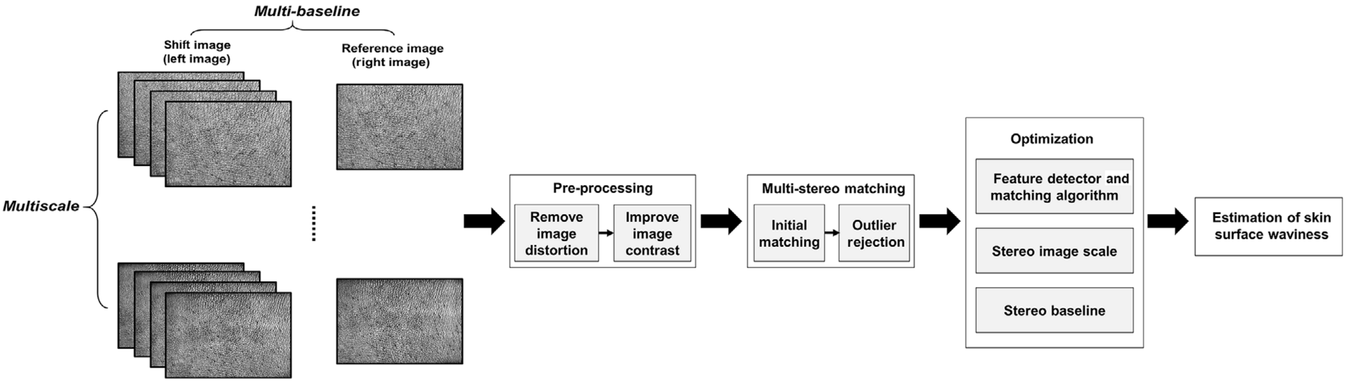

FIGURE 1 Overview of proposed three-dimensional (3D) skin analysis method in multiscale and multi-baseline. We acquired skin stereo images under multiscale, multi-baseline conditions using a mobile device. After preprocessing, stereo matching, and optimization, we performed optimal 3D analysis of the skin surface

accurate evaluation of skin surface roughness, it is effective to obtain skin information in the central region where the effect of skin curvature is small. Here, the baseline value of 10 mm is the maximum shifting distance that includes a flat skin region and has a stereo matching range suitable for surface roughness analysis. In addition, the polygonal size of the skin microstructure is less than 1 mm, so we set the minimum shifting distance to 1 mm. The acquired mobile images had dimensions of 2064 × 1548 pixels. The actual image size was 34.5 × 26 mm at a working distance of 60 mm, 37 × 28 mm at 65 mm, 39 × 29 mm at 70 mm, 41 × 31.5 mm at 75 mm, and 45 × 34 mm at 80 mm, respectively. Fifty pairs of stereo images were acquired for each subject. Thus, 400 mobile stereo image pairs were used in our study. To estimate the actual depth, we acquired a pair of stereo images of a standard bar, which is a material with a total height of 1 mm in units of 0.05 mm.

Conventionally, for stereo matching, rectification was performed to transform the image so that the epipolar line of the stereo image was parallel. However, the rectification process causes image distortion, which hiders the quantification of fine features such as skin microrelief and takes a long time. We have proven that 3D analysis of the stereo image is possible without rectification using the proposed mobile stereo system through the existing study.[21] Therefore, we performed skin microrelief analysis using the proposed method that improved the accuracy and speed of stereo matching without rectification.

2.2 | Skin microrelief depth estimation using stereo matching

We performed four steps for precision depth estimation of the skin microrelief: preprocessing, feature extraction, stereo matching, and real depth mapping. Figure 1 shows the entire process of 3D analysis of skin microrelief. We used MATLAB (R2019a, The MathWorks, Cambridge, UK) and OpenCV 3.3 for the preprocessing of the mobile image, image distortion correction, and stereo matching.

2.2.1 | Preprocessing

We performed two preprocessing steps for 3D image analysis: (1) image contrast improvement and (2) image distortion correction. The mobile skin image contains skin curvature and environmental noises such as illumination, reflection, and shadows. Therefore, the image is preprocessed to remove these noises and improve the contrast for accurate interpretation. In our previous studies, we acquired images of the skin with improved structural characteristics.[12] The mobile images include fine distortion so that the geometric distortion in the image causes errors, during stereo matching, in the disparity. This makes skin feature data less reliable. Hence, we corrected the mobile stereo images using the developed distortion correction matrix,[21] generated the final preprocessed images, and used them for stereo matching. Figure 2 shows that the original image and preprocessed (image contrast enhancement and distortion correction) stereo images obtained under the conditions of a working distance of 70 mm and a baseline of 4 mm. Figure 2A is images of a standard scalar bar, and Figure 2B is skin surface images. The hole region in the stereo image can be observed through distortion correction.

2.2.2 | Feature extraction and matching

The stereo disparity can be estimated using the corresponding points in the left and right images. The disparity value, that is, the 3D information, is calculated using the position difference of the horizontal coordinates of the corresponding points.[22] Therefore, these point extraction and matching algorithms are important for accurate and precise depth estimations. The skin surface structure consists of a network of similar polygons, which causes numerous errors in feature extraction. Thus, for accurate and precise stereo matching of skin surface images, we should use a change invariant and robust feature detector descriptor algorithm. We selected six local feature detector and descriptor algorithms, SIFT, SURF, BRISK, ORB, AKAZE, and ASFIT, and evaluated the performance of the skin feature extraction.

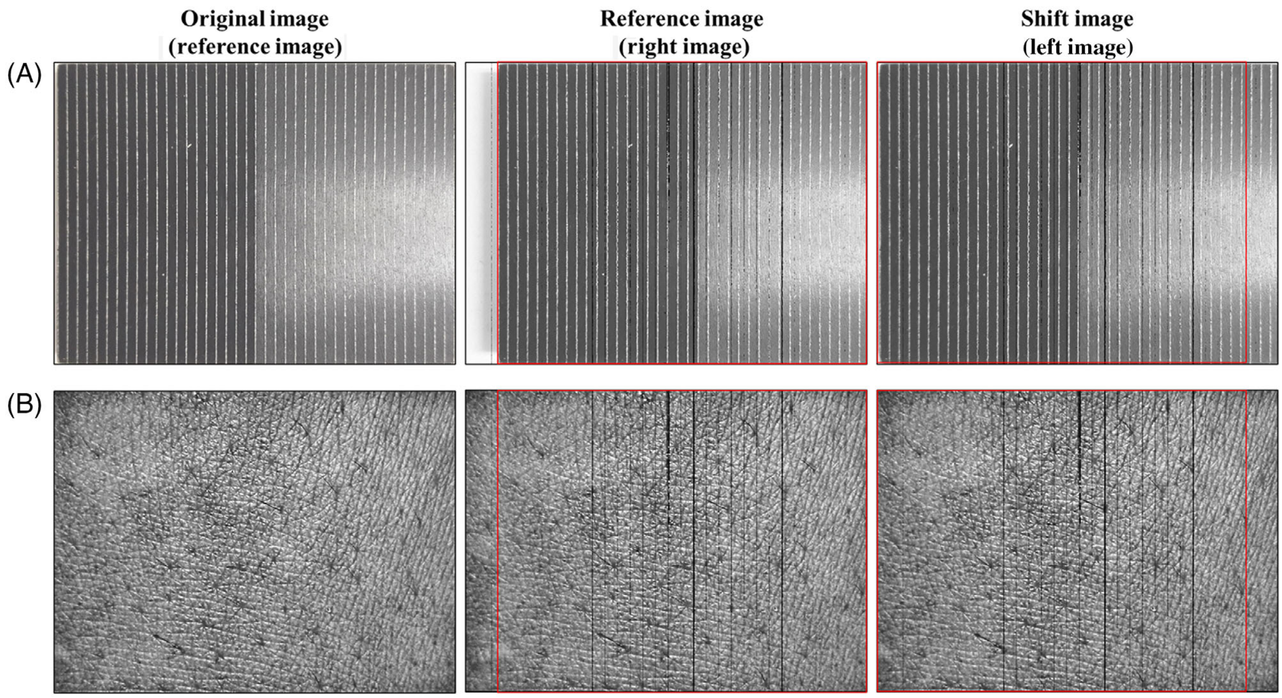

FIGURE 2 Mobile stereo images under the conditions of a working distance of 70 mm and a baseline of 4 mm: (A) stereo image of a standard scalar bar, (B) stereo image of skin surface. From the left, they are the original image and the preprocessed stereo images

TABLE 1 List of the stereo matching algorithms

Serial number	Feature extractor	Feature descriptor	Feature matching
1	SIFT	SIFT	FLANN
2	SURF	SURF	FLANN
3	ORB	ORB	BF
4	BRISK	BRISK	BF
5	AKAZE	AKAZE	BF
6	ASIFT	ASIFT	SIFT

Abbreviations: AKAZE, accelerated KAZE; BF, brute-force; FLANN, fast library for approximate nearest neighbor.

SIFT and SURF use a fast library for approximate nearest neighbor matching. ORB, BRISK, and AKAZE use brute-force matching, whereas ASIFT uses SIFT matching. Table 1 lists an additional comparison. We removed the matching points in the geometric error or correction interpolation regions as outliers.

2.2.3 | Depth mapping

We used a standard scalar bar that knows the height to verify the depth analysis performance using the proposed mobile stereo system. In the existing study,[21] we verified the 3D information extracted from the mobile stereo images of the standard scalar bar. In this study, we develop depth-mapping formulas in the micro-range using stereo images of a standard scalar bar acquired under the same conditions as skin imaging and estimate the actual depth of the skin microrelief using this. The standard scalar bar was 1 mm in height, with 20 engraved lines at 0.05-mm intervals. The disparity value differed based on the height. Therefore, we performed a multiple polynomial regression analysis on the relationship between the actual depth and disparity at each line (using the stereo images of the standard scalar bar) and calculated a second-order polynomial. We converted the disparity value, which is the skin stereo matching result, into the actual depth using depth-mapping formulas.

2.3 | Statistical processing

Minitab v19 (Minitab Inc., Coventry, UK) was used for the data analysis. We performed a multiple regression analysis of the actual depth and disparity and derived 50 depth-mapping formulas in accordance with the working distance and baseline. We then performed a one-way analysis of variance (ANOVA) on the results of the stereo matching algorithms for the performance evaluation of feature extraction and matching.

3 | RESULTS

3.1 | Proposal of real micro-range depth mapping

We used 50 depth-mapping formulas under multiscale, multi-baseline conditions, and analyzed the actual waviness of the skin surface. Theoretically, the disparity d, depth z, baseline b, and focal length f are

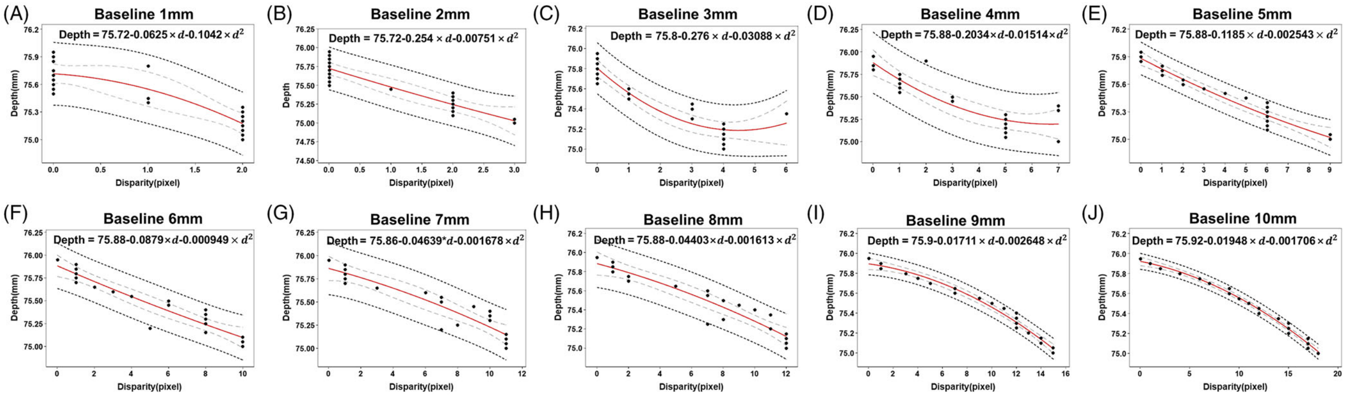

FIGURE 3 Quadratic polynomial regression formula for actual depth value. (A)~(J) graphs show the results of the multiple regression analysis of the relationship between disparity and actual depth for a standard scalar bar. (A)~(J) graphs indicate depth mapping formula under working distance of 75 mm and baseline of 1–10 mm. We converted the disparity to the actual depth using these formula.

related by $d = bf/z$, whereas d and z are nonlinearly related. However, our results did not show an ideal nonlinear relationship because the acquired mobile image has a high resolution and contains fine errors after distortion correction. Thus, we derived a second-order polynomial that can interpret the observed disparity as the actual depth.

Figure 3A–J shows micro-depth-mapping formulas for results of stereo matching at a working distance of 75 mm with a baseline of 1–10 mm. It confirmed the disparity differences according to the height differences at each line. In addition, for a larger baseline, sensitive depth differences were extracted that could provide better 3D information. In other words, with the increase in the baseline, we can extract precise 3D information. However, with the decrease in the range of stereo matching, the matching errors increase; the observation of various skin features becomes challenging. Therefore, it is necessary to find an optimal baseline to extract accurate and precise skin features. Using the proposed depth-mapping formulas, according to the baseline, we can conduct the actual depth estimation and 3D analysis of the skin surface under the optimal conditions, presented later. We list other depth-mapping formulas for working distances of 60, 65, 70, and 80 mm (shown in the Appendix).

3.2 | Stereo matching performance of skin surface images

We present a feature detector descriptor algorithm with the highest performance for skin feature (wrinkles, wrinkled cells) extraction and stereo matching. We aim to perform a quick and accurate 3D analysis using 3D points of the skin microrelief, excluding the process of disparity map generation. We evaluated the performance of six algorithms (SIFT, SURF, ORB, BRISK, AKAZE, and ASIFT). In stereo matching, the performance of the algorithm is measured by the number of features extracted and the accuracy of the match. When more features are extracted, the initial matching rate is higher, and thus, the algorithm performance is higher. Therefore, we evaluated how many algorithms can extract robust features that are invariant to scale, rotation, and affine changes. After excluding the outlier, we calculated the number of final matching points and matching rates for the six algorithms.

We performed stereo matching for the entire pair of stereo images acquired at each working distance and compared the performance of the algorithm using the average of the number of final matching points for each subject's data. The results of one-way ANOVA for the six algorithms confirmed the differences in algorithm performance ($p < 0.05$). Tukey's post-analysis test confirmed that AKAZE and ASIFT extracted more features than the other four algorithms, regardless of the image scale changes (Figure 4A). In other words, AKAZE exhibited the highest performance, whereas SURF exhibited the lowest performance in skin feature extraction. In addition, we evaluated the final matching rate. Figure 4B shows the number of matching points and corresponding matching rate at different working distances. AKAZE, ASIFT, BRISK, ORB, and SIFT generally exhibit good matching rates of 85%–90%. However, the matching rate of SURF was the lowest because the matching error increased with the stereo baseline. When the results were more distributed in the upper right part of the graph, the performance of the algorithm was higher. Thus, AKAZE and ASIFT were superior in terms of both the number of matching points and matching rate. Figure 4C shows the results of stereo matching in multiscale images according to the working distance when the baseline was 5 mm. In conclusion, mobile skin images not only contain viewpoint changes (baseline 1–10 mm) and various environmental noises (illumination and curvature), but also interpolation regions after distortion correction. Thus, numerous stereo-matching errors occur. Therefore, we selected the AKAZE algorithm, which proved to have better performance, to extract accurate and numerous skin features.

3.3 | Optimization of stereo image condition

Our study recommends an optimal image scale and baseline for the accurate observation and an analysis of the skin surface using

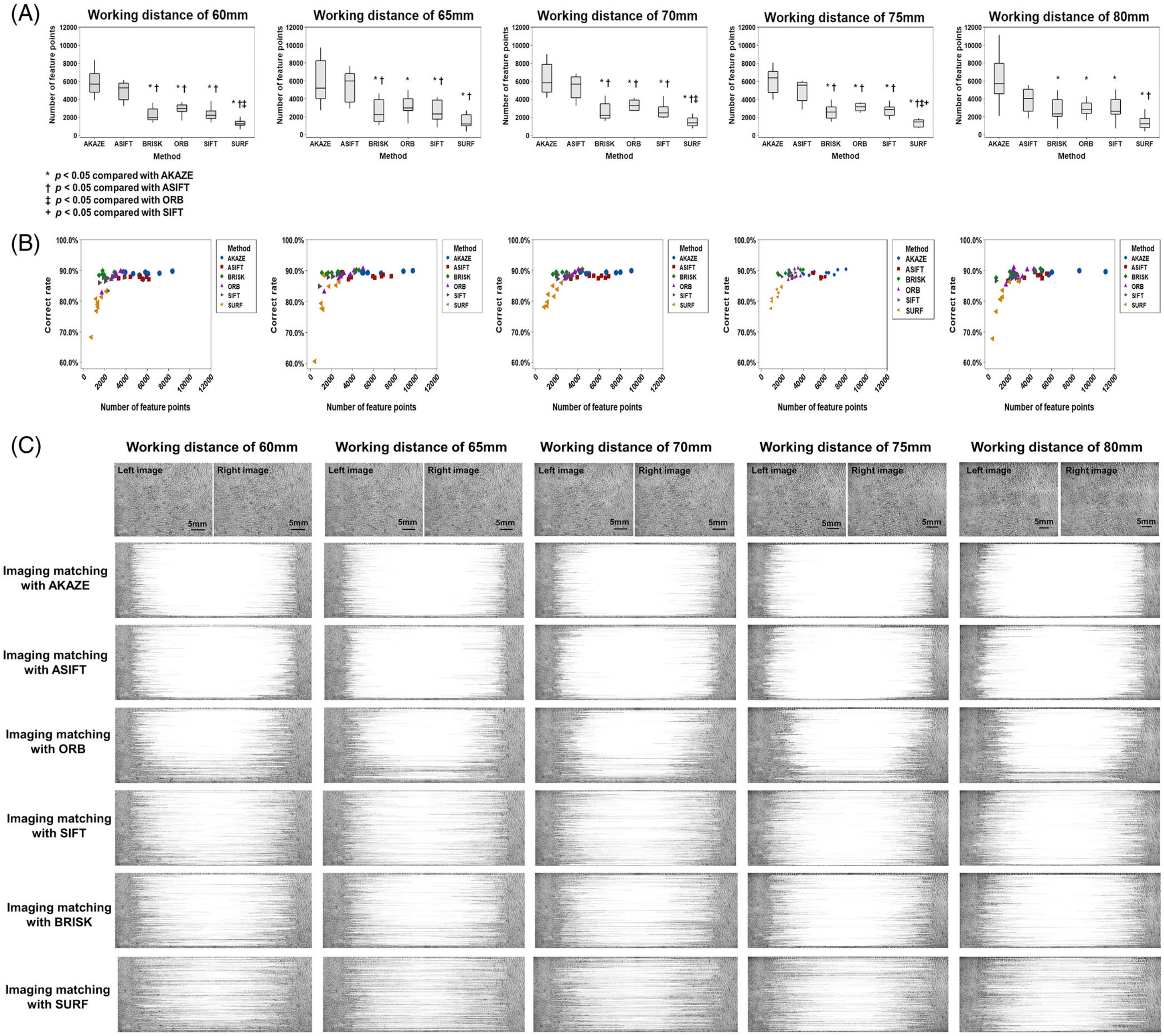

FIGURE 4 Performance evaluation of feature extraction and matching algorithms: (A) one-way analysis of variance (ANOVA) for differences among algorithms, (B) relationship between correct rate and number of feature points among algorithms, (C) matching results of algorithms for multiscale stereo images

multiscale and multi-baseline stereo images. First, a good scale condition implies the extraction of numerous matching points in the observation range. Based on the results of AKAZE, we confirmed the matching results (number of final matching points) for different scale images of the entire sample (Figure 5). The image scales (i.e., working distances) that provided the best results for each subject were different. However, more skin features are normally extracted at working distances of 70–75 mm. The extraction of numerous matching points indicated numerous distinct skin features within the observation range of the stereo image. We confirmed the distribution region of matching points in each zone by dividing the disparity range into four zones at each scale. Figure 6 shows the matching results of AKAZE when the baseline was 5 mm, and the disparity belonged to the low range (yellow). This implied that the skin surface was relatively deep. The opposite result was obtained when the disparity belonged to a high range (blue), which implied that the skin surface was relatively high. We could estimate the waviness of the skin surface using disparity analysis. In addition, for a wider disparity range, the depth information can be precisely interpreted. As shown in Figure 6, the center of the back of the hand or region leading to the fingers has a relatively high surface (cyan–blue range), whereas the regions on both ends of the hand have a low surface (yellow–green range). If the working distance is too small (working distance of 60 mm) or too large (working distance of 80 mm), it is difficult to detect the difference in the skin surface waviness, and the ambiguity region, such as the shadows on both ends of the image, increases. In conclusion, the images acquired at working distances of

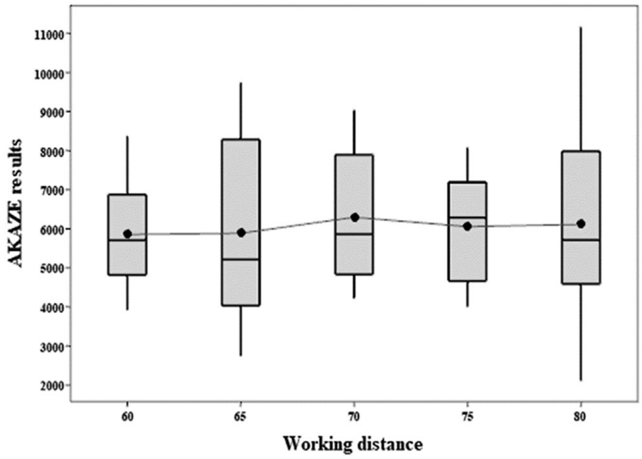

FIGURE 5 Comparison of the average number of final matching points of all subjects at each working distance. This graph shows the relationship between the final matching points using accelerated KAZE (AKAZE) and different working distances. The working distance is better when more matching points are matched. As shown in the graph, the best working distance is 70–75 mm

65–75 mm can be used to detect and extract distinct skin features and precisely identify skin surface waviness.

Next, we performed a comparative analysis of the baseline (1–10 mm) conditions using the AKAZE results of stereo images at a working distance of 75 mm. Figure 7B–K shows the disparity results when the baseline was 1–10 mm. As shown in the reference image (right image in Figure 7A), we can see the curvature of the skin surface with naked eye. It is important to find a proper baseline to interpret the surface curvature precisely. Thus, we recommend an optimal baseline by comparing and analyzing the disparity range and matching points that express the four disparity zones. When the baseline is 1–3 mm, it is challenging to detect the disparity accurately owing to the geometric error (after distortion correction) and precisely identify the surface waviness owing to the narrow disparity range. When the baseline was 9–10 mm, the detection features were not dense, and the disparity range was narrow. Dense skin features can be detected at a baseline 4–6 mm and identify the left region of the skin accurately based on the reference image at baselines of 7–8 mm. Consequently, when the baseline is 4–8 mm, the disparity can be densely extracted and the skin surface waviness can be accurately analyzed.

3.4 | Extracting 3D waviness information of the skin surface

Based on the previous results, we acquired mobile stereo images of the skin under optimal conditions (baseline: 7 mm, working distance: 75 mm) and performed stereo matching using AKAZE. We performed a surface waviness analysis by selecting skin data with distinct differences in the skin surface. Figure 8 shows the final matching results for the four subjects. The actual depth of the surface can be estimated using the proposed depth-mapping formula. Thus, we showed the results by calculating the actual depth using the extracted disparity. We did not observe large depth differences on the surface of the first row of relatively silky skin. The third and fourth rows exhibit differences in depth in the surface curvature region that is visible to the naked eye. In addition, when detailed depth differences appear in the disparity results, the roughness of a specific range of the skin surface can be analyzed using disparity analysis. We can compare 3D skin analysis for different skin surfaces using the calculated actual depths.

4 | DISCUSSION

Skin images acquired by mobile devices include fine distortions or various uncontrolled environmental noises, which hinder the acquisition of images and the analysis of skin features. In addition, previous studies had limitations in 3D analysis, such as the depth of wrinkles and roughness of the surface, owing to the use of 2D images only. To overcome the limitations of previous studies, we performed an optimization study for the 3D analysis of the skin surface using the stereo vision technique. We analyzed mobile skin stereo images (multiscale, multi-baseline) and showed the skin feature extraction and matching algorithm, image scale, and stereo baseline providing the highest performance. In conclusion, we performed a 3D analysis of the waviness of a skin surface using stereo matching.

We recommend three optimal methods for an accurate and precise analysis of mobile skin stereo images under multiscale and multi-baseline conditions. First, we evaluated the best algorithm for extracting skin surface features (wrinkles and wrinkled cells) and their matching. The structure of the skin surface consists of a fine and similar polygon, which leads to numerous stereo-matching errors. Therefore, we compared and evaluated the performance of six representative algorithms for skin feature extraction and matching. According to the number of final matching points and the matching rate, the following performances of the algorithms were obtained: AKAZE > ASIFT > ORB > BRISK > SIFT > SURF.

Second, we evaluated the mobile image scale to determine the best skin observation. According to the changes in the image scale, feature ambiguity by shadows or curvatures appears. These effects lead to sparser matching results and low precision of depth information. Therefore, it is important to select the image with the best scale for observing the skin surface. To select the image scale, we compared and analyzed the denseness of the matching points and precision of the skin surface waviness through the results of stereo matching at five working distances of 60–80 mm. Our results show that the best scale that enables the detection of additional matching points and details a precise surface waviness is from images acquired at a working distance of 70–75 mm.

Third, we evaluated the baseline stereo images for the most precise skin analysis. The expressed disparity range differed according to baseline. The disparity range is related to the precision of the 3D analysis. Therefore, to obtain the optimal baseline, we performed a comparative analysis of stereo images with a total of 10 steps at the baseline (1–10 mm). The criteria for the optimal baseline are the detection

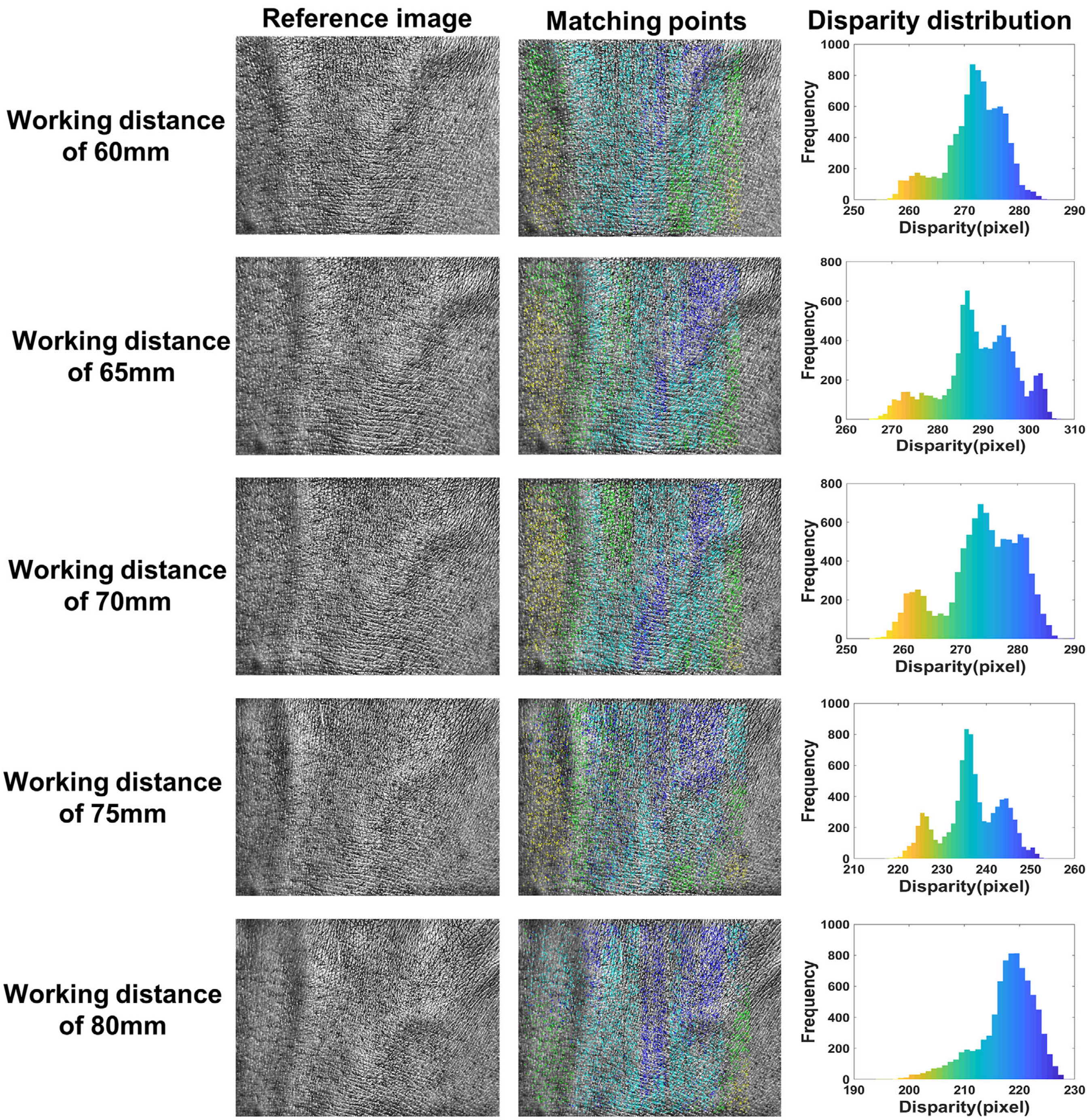

FIGURE 6 Disparity results of multiscale skin image. The stereo-matching results of accelerated KAZE (AKAZE), when the baseline is 5 mm under multiscale conditions is shown. The best image scale accurately and precisely expresses the waviness of the skin surface. The color-expressing disparity points in the second column confirm acceptable results for images acquired at working distances of 65–75 mm

of numerous matching points in the observation region and accurate estimation of waviness. When the baseline is too small (1–3 mm), the mobile skin image includes fine geometric errors (after mobile image distortion correction); the disparity range is narrow, which hinders a detailed analysis of the depth of the skin surface. Conversely, when the baseline is too large (9–10 mm), numerous matching errors occur, and thus, the number of detected matching points is small, which hinders accurate 3D analysis. Therefore, our study recommends a baseline range of 4–8 mm, which can be used to extract dense matching points and accurately express the surface waviness.

In this study, we developed a depth-mapping formula to estimate the actual depth using the disparity extracted under three proposed conditions for 3D skin analysis. We performed 3D analysis and evaluation of the waviness of the skin surface expressed in terms of actual depth.

We propose a 3D analysis method for the skin surface using an optimized mobile-based stereo system. It is possible to estimate and

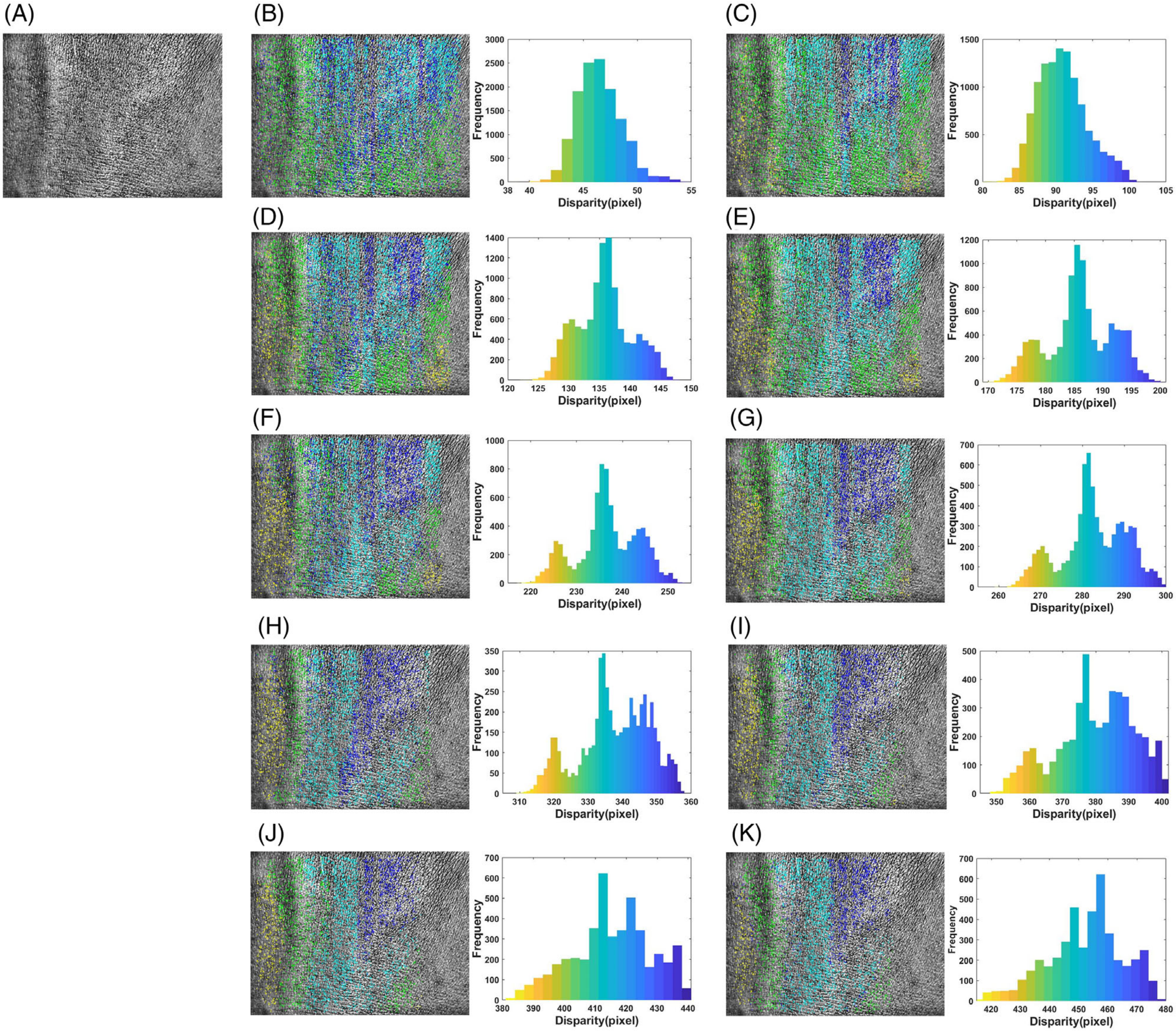

FIGURE 7 Disparity results of multi-baseline stereo images. The stereo matching results of accelerated KAZE (AKAZE), under multi-baseline conditions, when the working distance is 75 mm are shown. (A) is reference image, and (B)~(K) show the stereo matching results under baseline of 1-10 mm. When we confirm the color-expressing disparity points of (B-K), the skin waviness is expressed precisely at baselines of 4-8 mm (E-I)

analyze the actual fine curvature and waviness of the skin surface. In addition, the proposed method uses the 3D points of the skin instead of the disparity map for 3D analysis; thus, the performance is fast, accurate, and precise. Our method can be utilized in the analysis of various skin diseases, such as atopic dermatitis and psoriasis (from diseases with fine thickness to keloids with large shape and height). In addition, our method can be effectively used to perform 2D or 3D analyses regardless of the size of skin diseases, body curvature, and image shooting environment.

5 | CONCLUSIONS

Our study presents optimal conditions that enable 3D skin analysis using mobile devices to evaluate skin surface waviness. We can precisely observe the different skin surface curvatures. Previous studies did not optimize various stereo image conditions for the observation of skin surface features and had a limitation in the analysis range of the skin. However, we observed a wider skin surface and increased the accuracy of the skin analysis. In addition, the disparity map of the skin surface using stereo vision generated 3D information error; we used disparity values instead of disparity maps. Thus, we can quantify the 3D information of the local analysis of the skin as well as the global analysis. In addition, we suggest an actual depth-mapping formula to calculate the actual depth difference. In conclusion, we performed a 3D analysis of the micro-range using a multi-conditioned mobile stereo system that can be used in various fields. Our study was conducted on a limited age group in the 20s, but if future studies are conducted on different age groups, it is expected that new skin analyses, such as aging, will be observed.

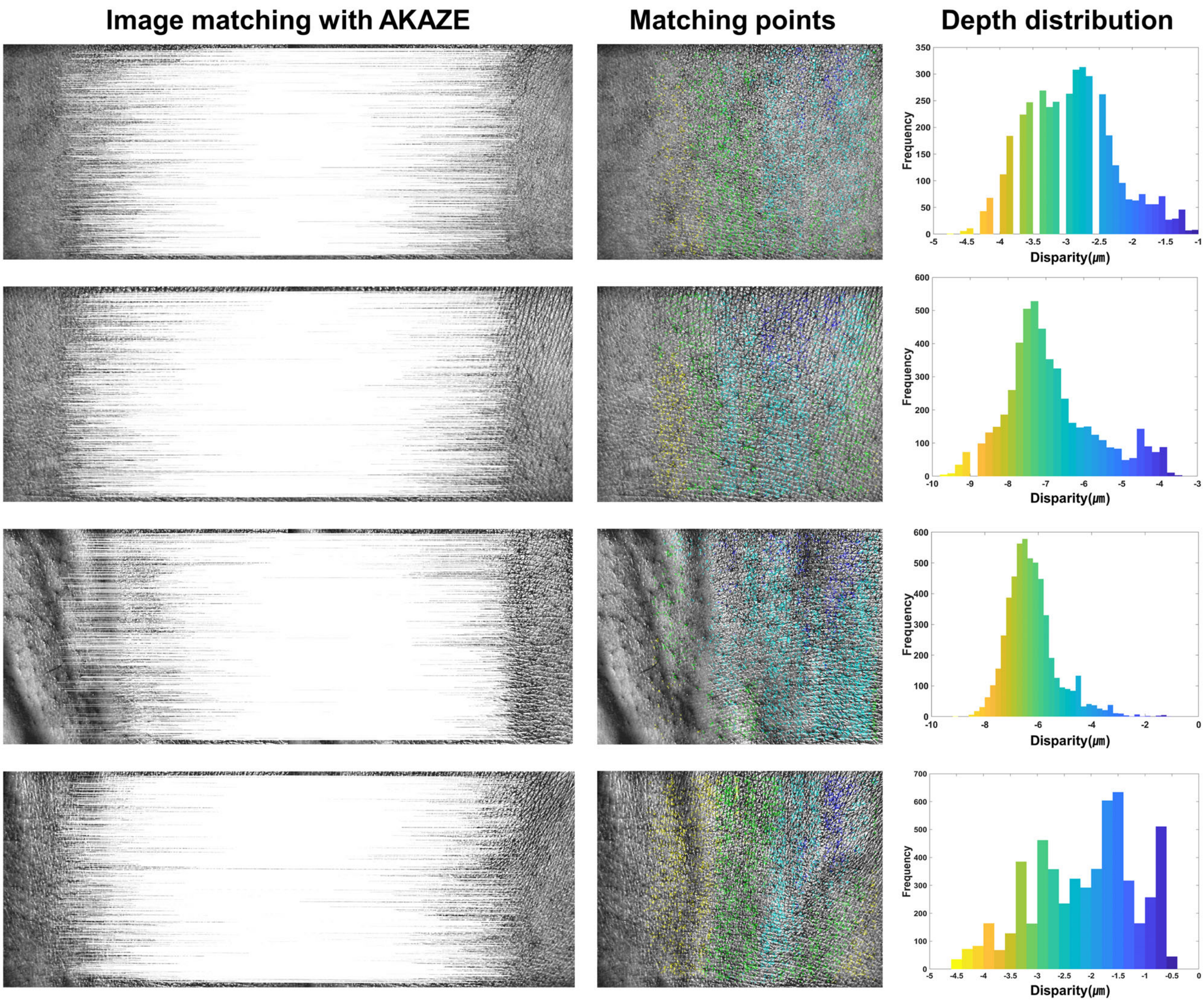

FIGURE 8 Depth analysis for different subject skin images. The three-dimensional (3D) skin analysis results for four subjects at a working distance of 75 mm and baseline of 7 mm are presented. The four skin images contain different skin characteristics, such as curvature and waviness of the skin surface. The figure shows the analysis results that reflect these skin characteristics. The actual depth of the matching point can be estimated by converting the calculated disparity to the actual depth

ACKNOWLEDGMENTS

This work was supported by the Soonchunhyang University Research Fund, BK21 FOUR (Fostering Outstanding Universities for Research) (5199990914048), and the National Research Foundation of Korea (NRF) grant funded by the Korea government (MSIT) (2022R1A2C1010170), and the Ministry of Education (No. 2020R1A6A3A13072938).

CONFLICT OF INTEREST

The authors state that they have no conflicts of interest.

DATA AVAILABILITY STATEMENT

Research data are not shared.

ORCID

Onseok Lee https://orcid.org/0000-0002-3696-9353

REFERENCES

1. Messaraa C, Metois A, Walsh M, et al. Wrinkle and roughness measurement by the Antera 3D and its application for evaluation of cosmetic products. *Skin Res Technol*. 2018;24(3):359-366.
2. Limbert G, Kuhl E. On skin microrelief and the emergence of expression micro-wrinkles. *Soft Matter*. 2018;14(8):1292-1300.
3. Callaghan T, Wilhelm KP. A review of ageing and an examination of clinical methods in the assessment of ageing skin. Part I: Cellular and molecular perspectives of skin ageing. *Int J Cosmet Sci*. 2008;30(5):313-322.
4. Askaruly S, Ahn Y, Kim H, et al. Quantitative evaluation of skin surface roughness using optical coherence tomography in vivo. *IEEE J Sel Top Quantum Electron*. 2018;25(1):1-8.
5. Moon C-I, Lee J, Yoo H, Baek Y, Lee O. Optimization of psoriasis assessment system based on patch images. *Sci Rep*. 2021;11(1):1-13.
6. Somthong T, Yang Q. Average surface roughness evaluation using 3-source photometric stereo technique. *Int J Metrol Qual Eng*. 2016;7(4):406.

7. Korotkov K, Quintana J, Campos R, et al. An improved skin lesion matching scheme in total body photography. *IEEE J Biomed Health Inform*. 2018;23(2):586-598.
8. Lee O, Lee G, Oh J, Kim M, Oh C. An optimized in vivo multiple-baseline stereo imaging system for skin wrinkles. *Opt Commun*. 2010;283(23):4840-4845.
9. Skvara H, Burnett P, Jones J, Duschek N, Plassmann P, Thirion JP. Quantification of skin lesions with a 3D stereovision camera system: validation and clinical applications. *Skin Res Technol*. 2013;19(1):e182-e190.
10. Rew J, Choi Y-H, Kim H, Hwang E. Skin aging estimation scheme based on lifestyle and dermoscopy image analysis. *Appl Sci*. 2019;9(6):1228.
11. Wu Y, Tanaka T. Objective and quantitative measurement of skin micro-relief by image analysis and application in age-dependent changes. *Skin Res Technol*. 2021;27(6):1072-1080.
12. Moon CI, Lee O. Age-dependent skin texture analysis and evaluation using mobile camera image. *Skin Res Technol*. 2018;24(3):490-498.
13. Hong G, Lee O. Three-dimensional reconstruction of skin disease using multi-view mobile images. *Skin Res Technol*. 2019;25(4):434-439.
14. Moon C-I, Lee O. Skin microstructure segmentation and aging classification using CNN-based models. *IEEE Access*. 2021;10:4948-4956.
15. Lowe DG. Distinctive image features from scale-invariant keypoints. *Int J Comput Vision*. 2004;60(2):91-110.
16. Bay H, Ess A, Tuytelaars T, Van Gool L. Speeded-up robust features (SURF). *Comput Vision Image Understanding*. 2008;110(3):346-359.
17. Leutenegger S, Chli M, Siegwart RY. BRISK: binary robust invariant scalable keypoints. Paper presented at: 2011 International Conference on Computer Vision. 2011.
18. Rublee E, Rabaud V, Konolige K, Bradski G. ORB: an efficient alternative to SIFT or SURF. Paper presented at: 2011 International Conference on Computer Vision. 2011.
19. Yu G, Morel J-M. ASIFT: an algorithm for fully affine invariant comparison. *Image Process Online*. 2011;1:11-38.
20. Alcantarilla PF, Solutions T. Fast explicit diffusion for accelerated features in nonlinear scale spaces. *IEEE Trans Pattern Anal Mach Intell*. 2011;34(7):1281-1298.
21. Moon C-I, Lee O. Adaptive fine distortion correction method for stereo images of skin acquired with a mobile phone. *Sensors*. 2020;20(16):4492.
22. Hamid MS, Abd Manap N, Hamzah RA, Kadmin AF. Stereo matching algorithm based on deep learning: a survey. *J King Saud Univ—Comput Inf Sci*. 2022;34(7):1663-1673.

How to cite this article: Moon C-I, Lee O, Choi M-H. Robust skin microrelief depth estimation using a mobile stereo system. *Skin Res Technol*. 2022;28:815–826. https://doi.org/10.1111/srt.13204

APPENDIX

Quadratic polynomial regression formula for actual depth value at the working distance 60, 65, 70, and 80 mm.